Proceedings of the 16th International Conference on Soil Mechanics and Geotechnical Engineering

doi:10.3233/978-1-61499-656-9-811

Numerical modeling of the anisotropic stress-strain behavior of granular soils based on the micromechanics theory

Modeler numérique du comportement anisotrope de contrainte-tension des sols granuleux basés sur la théorie de micromécanique

Young-Hoon Jung, Choong-Ki Chung & Myoung-Mo Kim
School of Civil, Urban and Geo-system Engineering, Seoul National University, Korea

ABSTRACT

Granular soils can be perceived as a collection of discrete particles. In this study, a numerical modeling and analysis of the anisotropic stress-strain behavior of granular soils based on the micromechanics theory were attempted. A new program employing the nonlinear contact stiffness model obtained from experimental data on metallic materials was developed. The numerical results indicated that the nonlinear contact force-displacement relationship, under isotropic stress condition, manifested itself as a pressure-dependent elastic moduli. For the anisotropic stress condition, the elastic and the elastic-plastic behavior of granular soils were essentially affected by both the nonlinear contact stiffness and the evolution of fabric anisotropy during shearing.

RÉSUMÉ

Les sols granuleux peuvent être considérés comme des assemblages de particules discrètes. Cette étude propose un modèle ainsi qu'une analyse numériques du comportement contrainte-déformation basés sur une théorie à l'échelle micromécanique. Un programme exploitant un modèle non-linéaire de rigidité aux points de contact est développé à l'aide de résultats expérimentaux obtenus pour des matériaux métalliques. Au vu des résultats numériques, il apparaît que la relation force-déplacement au point de contact soumis à contrainte isotropique se manifeste sous la forme de modules d'élasticité dépendant de la pression. Sous contrainte anisotropique, le comportement élastique et élasto-plastique des sols granuleux est essentiellement fonction de la rigidité non-linéaire au point de contact et de l'évolution de l'anisotropie inhérente de fabrique lors du cisaillement.

1 INTRODUCTION

Granular soils can be regarded as a collection of discrete particles. The overall mechanical properties of granular materials are significantly dependent on the packing structure and mutual interaction at the particle contacts. The anisotropic characteristics of macroscopic stress-strain responses of granular soils are closely related to the spatial distribution of linkage between the contacts. The micromechanics theory dealing with the interaction of particles provides a useful way to estimate the complex stress-strain behavior of granular soils. Recent experimental studies on the elastic properties of anisotropic soils (Bellotti et al., 1996; Kuwano and Jardine, 2002) also emphasize the potential of micromechanical approaches.

In this research, the numerical modeling and analysis of the anisotropic stress-strain behavior of granular soils was attempted based on the micromechanics theory. To derive the macroscopic constitutive equation, the homogenization technique was used because it can give a consistent result regardless of the number of particles in the soil assembly. A micromechanics-based program incorporating the nonlinear contact stiffness model and the explicit expression for evolution of fabric anisotropy was developed. A procedure to obtain the model parameters at micro-scale from measured experimental data is presented. The results of model estimation were compared with test data on Ham River sand performed by Kuwano and Jardin (2002). This study aimed to simulate and understand the nonlinear and anisotropic behavior of elastic and elastic-plastic responses with a proper consideration of the particulate nature of granular soils.

2 MICROMECHANICS MODEL

A numerical program based on the micromechanics theory was developed to investigate the nonlinear anisotropic stiffness of granular soils. It was assumed that there are no loss or gain of the number of contacts, no particle spinning and no resisting moment at the contact points during deformation. The soil mass was idealized as an assembly of mono-sized spheres with cross-anisotropic fabric. Despite the idealized shape of spheres within the assembly, the local irregularity on the contact surface was taken into account to formulate the contact stiffness.

2.1 *Nonlinear contact stiffness model*

The microscopic contact model defines the basic relations between contact forces and contact displacements in a contact plane generated by two neighboring particles. With the assumption of no angular displacements and no coupling between the forces or displacements in the normal and tangential directions, the contact stiffness model can be defined as

$$\begin{Bmatrix} \delta f_n \\ \delta f_s \\ \delta f_t \end{Bmatrix} = \begin{bmatrix} k_n^{el} & 0 & 0 \\ 0 & k_r^{el} & 0 \\ 0 & 0 & k_r^{el} \end{bmatrix} \begin{Bmatrix} \delta d_n^{el} \\ \delta d_s^{el} \\ \delta d_t^{el} \end{Bmatrix} \;\&\; \begin{Bmatrix} \delta f_n \\ \delta f_s \\ \delta f_t \end{Bmatrix} = \begin{bmatrix} k_n^{ep} & 0 & 0 \\ 0 & k_r^{ep} & 0 \\ 0 & 0 & k_r^{ep} \end{bmatrix} \begin{Bmatrix} \delta d_n \\ \delta d_s \\ \delta d_t \end{Bmatrix} \quad (1)$$

where δf_i = the increment of contact force acting on the contact plane, δd_i = the increment of contact displacement. The subscript n represents the normal direction in the contact plane, whereas s and t denote the two tangential directions. To investigate both elastic and elastic-plastic behaviors, the elastic components of contact displacements, δd_i^{el}, were differentiated from the total contact displacement, δd_i. Accordingly, k_n^{el} and k_r^{el} are the elastic contact stiffnesses in the normal and tangential directions on the contact plane, respectively. k_n^{ep} and k_r^{ep} denote the elastic-plastic contact stiffnesses related to the total contact displacement.

The normal contact stiffnesses k_n^{el} and k_n^{ep} are substantially affected by the geometry of the contact surface. Generally, a soil particle has a significant degree of irregularity on its surface. Thus, the idealization of soil particles' surfaces to establish the contact stiffness model was inevitable. For the metallic materi-

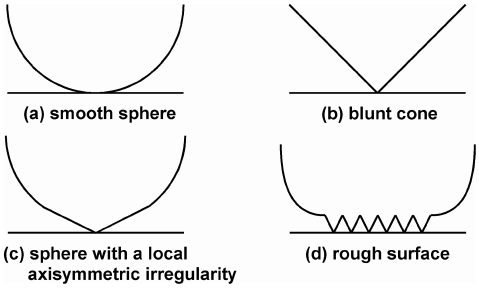

Figure 1. Different geometries of contact surfaces

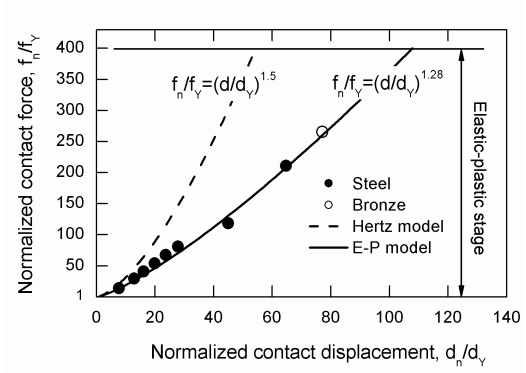

Figure 2. Normalized force-displacement relation at the elastic-plastic stage (data obtained from Johnson (1985))

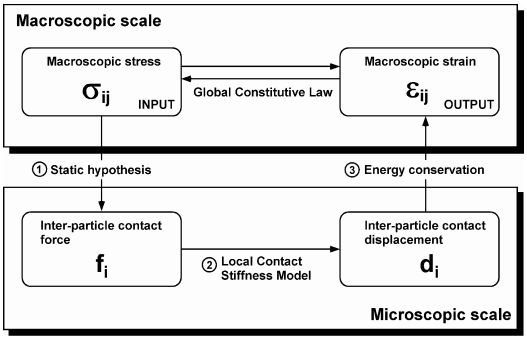

Figure 3. Analysis procedure for static hypothesis

als, a number of researchers suggested the expressions of the normal contact stiffness. As illustrated in Fig. 1, the idealized geometry for the axisymmetric contact surface can be classified into four types: i) smooth sphere (Hertz, 1882); ii) blunt cone (Johnson, 1985; Goddard, 1990); iii) sphere with a local axisymmetric irregularity (Jäger, 1999); iv) rough surface (Yimsiri and Soga, 2000). Jung (2004) compared the various expressions of k_n^{el} and found that irrespective of the geometry of the contact surface the elastic contact stiffness in the normal direction can be generalized as:

$$k_n^{el} = C_n^{el} (f_n)^{\alpha_n^{el}} \tag{2}$$

where C_n^{el} and α_n^{el} are the material constants. For the assembly under the isotropic pressure, the exponent α_n^{el} is directly related to the pressure-dependency of macroscopic elastic modulus and its value is about 0.5 for granular soils (Jung, 2004; Jung and Chung, 2004). This implies that the geometry of contact surface for granular soils approximates the blunt cone.

The elastic-plastic contact stiffness, k_n^{ep}, was formulated from experimental data concerning metallic materials. After the internal stress at a specific point within the contact body reached the yield strength of the material, the yielding of contact was initiated while the deformation of contact did not reach the fully plastic stage where the brittle particles would be crushed. At this stage of loading, the elastic-plastic contact stiffness could be formulated using the experimental data for the metallic materials. Fig. 2 shows the normalized force-displacement relation at the elastic-plastic stage experimentally observed by Johnson (1985). For the blunt conical contact, the maximum contact force to initiate yielding (f_Y), and the corresponding displacement (d_Y) can be derived as follows (Jung, 2004):

$$f_Y = \frac{\pi r_c^2}{8} \frac{(1-\nu_m)^2}{G_m^2} Y^3 \text{ and } d_Y = \frac{\pi r_c}{4} \frac{(1-\nu_m)^2}{G_m^2} Y^2 \tag{3}$$

where r_c = the radius of contact area, G_m and ν_m = the shear modulus and the Poisson's ratio of particle respectively, and Y = the yield stress of material. Herein, it was assumed that the contact force-displacement relationship at the elastic-plastic stage can be established via an exponential function such as:

$$f_n / f_Y = (d_n / d_Y)^{\theta} \tag{4}$$

where the value of θ (= 1.28) was obtained from the regression analysis shown in Fig. 2. The elastic-plastic contact stiffness can be formulated by differentiating Eq. (4), given by

$$k_n^{ep} = \frac{\theta (f_Y)^{1/\theta}}{d_Y} (f_n)^{(\theta-1)/\theta} = C_n^{ep} (f_n)^{\alpha_n^{ep}} \tag{5}$$

where C_n^{ep} and α_n^{ep} are the material constants and the value of α_n^{ep} is 0.22 for the given value of θ (= 1.28). With the assumption of no slip on the contact plane, the elastic contact stiffness in the tangential direction, k_r^{el} was defined as

$$k_r^{el} = C_r^{el} k_n^{el} \tag{6}$$

where C_r^{el} is the material constant and C_r^{el} =2(1- ν_m)/(2- ν_m) for the idealized spherical contact (Johnson, 1985). Based on the Hert-Mindlin theory (Mindlin and Deresiewicz, 1953), the elastic-plastic contact stiffness in the tangential direction, k_r^{ep}, was formulated by

$$k_r^{ep} = k_r^{el} (1 - f_r / f_n \tan\phi_m)^{\alpha_r^{ep}} \tag{7}$$

where ϕ_m = the inter-particle friction angle and α_r^{ep} = the material constant. For a spherical contact, the value of α_r^{ep} is 1/3. However, Walton and Braun (1986) reported that α_r^{ep} is larger than 1/3 for the non-spherical contact.

2.2 *Micromechanics-based program*

Using the static hypothesis (Emeriault and Chang, 1997; Yimsiri and Soga, 2000), the contact forces can be evaluated from the macroscopic stresses acting on the boundaries of the soil assembly. Fig. 3 illustrates the analysis procedure of the static hypothesis. Details of the program can be found in Jung (2004).

To consider the anisotropic nature of granular soils, the fabric tensor, a representative index of the packing structure that describes the spatial distribution of contact normal, was introduced into the numerical program. According to Oda and Nakayama (1998), the fabric tensor, F_{ij}, is defined as:

$$F_{ij} = \int_0^{2\pi} \int_0^{\pi} n_i n_j E(\gamma) \sin\gamma \, d\gamma \, d\beta \tag{8}$$

where n_i denotes the contact normal in the *i*-direction in the global coordinate system, $E(\gamma)$ the distribution function of contact normals, and γ and β represent the angles of position of a particular contact point in the spherical coordinate system. For the cross-anisotropic assembly, Chang et al. (1989) suggested the distribution function for the fabric tensor, given by

$$E(\gamma) = 3(1 + a\cos 2\gamma) / 4\pi(3 - a) \tag{9}$$

where a single parameter a, namely the degree of fabric anisotropy, controls the overall distribution of contact normals within a cross-anisotropic structure.

Table 1. Input parameters of the micromechanics-based program

Category	Input parameters		Values*
Contact Stiffness Model	C_n^{el}	for k_n^{el} (elastic)	15665 (13775)
	α_n^{el}		0.50
	C_r^{el}	for k_r^{el} (elastic)	0.817
	C_n^{ep}	for k_n^{ep} (elastic-plastic)	514 (452)
	α_n^{ep}		0.22
	α_r^{ep}	for k_r^{ep} (elastic-plastic)	3.0
	ϕ_m	Inter-particle friction angle	26 deg.
Contact Density	e_0	Initial void ratio	0.658
	r_m	Equivalent radius of particles	0.135mm
Contact Orientation	a_0	Initial value of a	0.171 (-0.224)
	a_1	Inclination of a-(q/p)line	0.34

* The values in parentheses are determined using a0 for the G_{hh}/G_{vh}.

Table 2. Material constants for the empirical expressions

Modulus	C (MPa)	a	b	a+b
E_v^{el}	204 (208)*	0.52	0.00	0.52 (0.50)
E_h^{el}	174 (179)*	0.00	0.53	0.53 (0.50)
G_{vh}^{el}	72 (73)*	0.32	0.20	0.52 (0.50)
G_{hh}^{el}	81 (80)*	-0.04	0.53	0.50 (0.50)

* The values in parentheses are the corrected values for the same exponent of a+b = 0.50.

To implement the evolution of fabric anisotropy, it was assumed that the value of a linearly increases from the initial value a_0 related the initial stress condition as the principal stress ratio q/p' increases during shearing. The expression for a is given by

$$a = a_0 + a_1(q/p') \tag{10}$$

where a_1 denotes the slope of increasing a with the principal stress ratio. Table 1 summarizes the input parameters of the numerical program.

3 DETERMINATION OF MODEL PARAMETERS

The parameters for the contact stiffness model are at the contact level and they were difficult to quantify from the laboratory test. If the analytical solutions that link the microscopic contact model and the macroscopic elastic moduli are established, the required parameters will be obtained using the empirical expressions of the cross-anisotropic elastic moduli (Kuwano and Jardine, 2002) as:

$$E_v^{el} = C_v f(e)(\sigma'_v/p_r)^{a_v}(\sigma'_h/p_r)^{b_v} \tag{11a}$$

$$E_h^{el} = C_h f(e)(\sigma'_v/p_r)^{a_h}(\sigma'_h/p_r)^{b_h} \tag{11b}$$

$$G_{vh}^{el} = C_{vh} f(e)(\sigma'_v/p_r)^{a_{vh}}(\sigma'_h/p_r)^{b_{vh}} \tag{11c}$$

$$G_{hh}^{el} = C_{hh} f(e)(\sigma'_v/p_r)^{a_{hh}}(\sigma'_h/p_r)^{b_{hh}} \tag{11d}$$

where C_v, C_h, C_{vh} and C_{hh} = the material constants, a_v, b_v, a_h, b_h, a_{vh}, b_{vh}, a_{hh} and b_{hh} = the moduli exponents indicating the pressure-dependency of elastic moduli, p_r = a reference pressure taken as atmospheric pressure (101.3kPa), σ'_v and σ'_h the vertical and horizontal effective stresses respectively, and the void ratio function $f(e) = (2.17-e)^2/(1+e)$. These relations can be established using the relevant laboratory data. For the isotropic stress condition, the approximate solutions of the elastic moduli using the cross-anisotropic fabric tensor and the nonlinear contact model can be derived as explained by Jung (2004) and detailed below:

$$E_v^{el} = C_n^{el}C_r^{el}\left[\frac{28r_m^2n_v(5+a_0)^2}{5(3-a_0)\{14-2a_0+C_r^{el}(21+9a_0)\}}\right]\left[\frac{5(3-a_0)}{2r_mn_v(5-3a_0)}\right]^{\alpha_n^{el}}(\sigma'_c)^{\alpha_n^{el}} \tag{12a}$$

$$E_h^{el} = C_n^{el}C_r^{el}\left[\frac{28r_m^2n_v(5-3a_0)^2}{5(3-a_0)\{14-6a_0+C_r^{el}(21-15a_0)\}}\right]\left[\frac{5(3-a_0)}{2r_mn_v(5-3a_0)}\right]^{\alpha_n^{el}}(\sigma'_c)^{\alpha_n^{el}} \tag{12b}$$

$$G_{vh}^{el} = C_n^{el}C_r^{el}\left[\frac{14r_m^2n_v(5-3a_0)^2(5+a_0)^2}{5(5-a_0)(3-a_0)\{105-46a_0-23a_0^2+C_r^{el}(70-24a_0+2a_0^2)\}}\right]\left[\frac{5(3-a_0)}{2r_mn_v(5-3a_0)}\right]^{\alpha_n^{el}}(\sigma'_c)^{\alpha_n^{el}} \tag{12c}$$

$$G_{hh}^{el} = C_n^{el}C_r^{el}\left[\frac{14r_m^2n_v(5-3a_0)^2}{5(3-a_0)\{21-11a_0+C_r^{el}(14-10a_0)\}}\right]\left[\frac{5(3-a_0)}{2r_mn_v(5-3a_0)}\right]^{\alpha_n^{el}}(\sigma'_c)^{\alpha_n^{el}} \tag{12d}$$

where r_m = the equivalent radius of particles, n_v = the contact density or the average number of contact points per unit volume, and σ'_c = the isotropic pressure. If all the values of a+b in Eq. (11) are the same under isotropic stress condition, the direct comparison of Eqs. (11) and (12) yields the values of the micromechanics parameters. After determining C_r^{el} with ν_m based on Hertz theory, the value of a_0 can be obtained by comparing the moduli ratio (i.e. E_h^{el}/E_v^{el} or G_{hh}^{el}/G_{vh}^{el}) from empirical expressions with that from micromechanical solutions. With the estimated values of C_r^{el} and a_0, the comparison of Eqs. (11) and (12) yields four values of C_n^{el} that should be the same theoretically. The values of α_r^{ep} and a_1 were determined using the parametric studies because there are no definite values for them.

In this study, the testing data on Ham River Sand reported by Kuwano and Jardine (2002) were used to evaluate the model parameters. Their results for establishing Eq. (11) are summarized in Table 2. For the direct comparison between Eqs. (11) and (12), it is necessary to correct the material constants of empirical expressions for the same exponent of a+b = 0.50. The corrected values are also summarized in Table 2. Table 1 gives the values of input parameters using the evaluation procedure explained by Jung (2004). The different sets of parameters are presented in Table 1 due to the inconsistent measurement of initial degree of anisotropy (i.e. E_h^{el}/E_v^{el} = 0.85 but G_{hh}^{el}/G_{vh}^{el} =1.13 in the isotropic stress condition). Because there was no reasonable solution to this discrepancy at the time, both sets of parameters were employed to compute the macroscopic elastic and elastic-plastic moduli. The parameters based on a_0 =0.171 for E_h^{el}/E_v^{el} and a_0 =-0.224 for G_{hh}^{el}/G_{vh}^{el} were selectively applied for predicting the soil behavior.

4 ANALYSIS OF NONLINEAR ANISOTROPIC BEHAVIOR OF GRANULAR SOILS

The numerical analyses were performed to investigate the nonlinear anisotropic behavior of granular soils from the micromechanics viewpoint. The triaxial compression tests were simulated by applying the boundary stress in the vertical direction from the initial condition of specimen under the isotropic stress of 200 kPa. During the isotropic consolidation, it can be found that the nonlinear contact stiffness manifests itself as the pressure-dependent responses of elastic moduli, judging from the similarity between Eq. (11) and Eq. (12). In the isotropic stress condition, the contact stiffness with pressure dependency is likely the unique factor to explain the nonlinear elastic behavior.

During the anisotropic loading, however, the above explanation would not be enough to describe the nonlinear elastic behavior. Fig. 4 compares the variation of elastic moduli during shearing under the conditions of i) constant degree of fabric anisotropy (Fig. 4(a)) and ii) varying degree of fabric anisotropy (Fig. 4(b)) where a_0 =0.171 was used for Young's moduli and a_0 = -0.224 served for shear moduli. Apparently, there are discrepancies between the computed results and the test data for the constant a condition. These anomalous results can be improved by considering the evolution of fabric anisotropy during

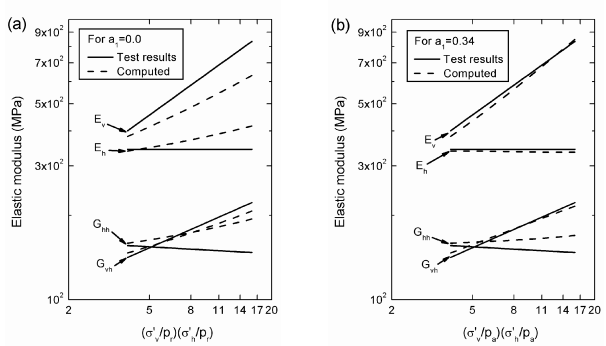

Figure 4. Variation of elastic moduli during shearing: (a) for the constant a; (b) for the varying a

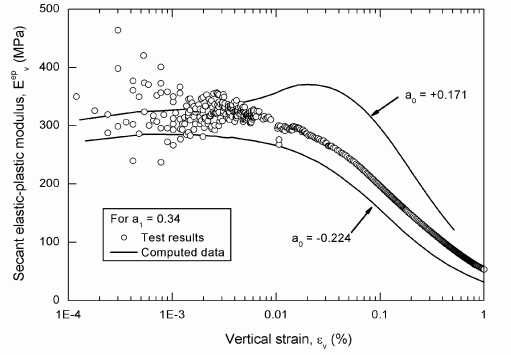

Figure 5. Variation of E_v^{ep} during shearing

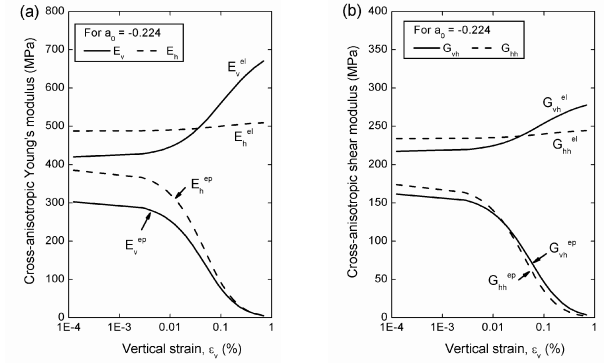

Figure 6. Variation of elastic and elastic-plastic moduli during shearing: (a) Young's moduli; (b) shear moduli

shearing with a_1 =0.34 obtained from a series of parametric studies, as shown in Fig. 4(b). Consequently, we concluded that the nonlinear elastic behavior should be explained not only by the pressure-dependent nature of the elastic moduli in the isotropic stress condition but also the simultaneous evolution of fabric anisotropy under the anisotropic loading.

The micromechanical prediction of elastic-plastic moduli provided additional information on the macroscopic behavior when the strains exceeded the pseudo-elastic limit. Fig. 5 compares the test data and the numerical results of the secant elastic-plastic moduli of E_v^{ep} for a_0 = 0.171. The model estimation of E_v^{ep} for a_0 = -0.224 was also plotted to investigate the effect of the initial degree of anisotropy during shearing.

For the positive value of a_0 (i.e. a_0 = 0.171) that means the vertically stiffer response in the isotropic stress condition, the increasing pattern of E_v^{ep} appeared at the small strains. The similar pattern of increasing stiffness was observed in an other experimental study reported by Kohata et al. (1997). The increase of E_v^{ep} during axial compression appeared as a distinctive feature of the stress-strain response for the initial fabric condition with positive a_0. In this case, however, the real value of a_0 may be negative because the experimental result did not indicate the apparent increase of modulus and the computed result with a_0 = -0.224 yielded the similar pattern of stiffness degradation, even though it gave the slightly reduced values of E_v^{ep}. These results emphasized the importance of initial state of fabric on the elastic-plastic behavior and the necessity of further experimental investigation for the accurate evaluation of the degree of fabric anisotropy. Fig. 6 provides the computed variations of the elastic and elastic-plastic moduli during triaxial compression for a_0 = -0.224. These results elucidated the possibility of using the micromechanical approach to describe both the nonlinear and the cross-anisotropic behavior of granular soils.

5 CONCLUSIONS

To investigate the nonlinear anisotropic behavior of granular soils, s micromechanics-based program was developed. The program introduced the nonlinear contact stiffness model and allowed the evolution of fabric anisotropy under anisotropic stress condition. A methodology for evaluating model parameters using a set of the analytical solutions of the elastic moduli in the isotropic stress condition was explained. The elastic and the elastic-plastic behavior of the soils were simulated based on the micromechanics theory. The numerical results compared with testing data emphasized the importance of fabric anisotropy and confirmed the usefulness of the micromechanics model to explain the nonlinear anisotropic characteristics of soil stiffness.

REFERENCES

Bellotti, R., Jamiolkowski, M., Lo Presti, D.C.F. and O'Neill, D.A. 1996. Anisotropy of small strain stiffness in Ticino sand. *Geotechnique*, 46(1), 115-131.

Chang, C.S., Sundaram, S.S. and Misra, A. 1989. Initial moduli of particulated mass with frictional contacts. *Int. J. for Numerical and Analytical Methods in Geomechanics*, 13, 629-644.

Emeriault, F. and Chang, C.S. 1997. Interparticle forces and displacements in granular materials. *Computers and Geotechnics*, 20(3/4), 223-244.

Goddard, J.D. 1990. Nonlinear elasticity and pressure-dependent wave speeds in granular media. *Proc. of Royal Society of London*, 430,105-131.

Hertz, H. 1882. Uber die Beruhrung fester elastischer Korper (On the contact of elastic solids). *J. reine und angewandte Mathematik,* 92, 156-171.

Jäger, J. 1999. Uniaxial deformation of a random packing of particles. *Archive of Applied Mechanics,* 69, 181-203.

Johnson, K.L. 1985. *Contact mechanics*. Cambridge University Press.

Jung, Y-H. 2004. Modeling of Nonlinear Anisotropic Deformation of Granular Soils in Pre-failure Condition by Numerical Approach. *Ph.D. dissertation*, Seoul National University.

Jung, Y-H. and Chung, C-K. 2004. Micromechanics Modeling and Analysis on Elastic behavior of Cross-anisotropic Granular Soils in Pre-failure Condition. *Int. J. for Numerical and Analytical Methods in Geomechanics* (submitted).

Kohata, Y., Tatsuoka, L., Wang, L., Jiang, G.L., Hoque, E. and Kodaka, T. 1997. Modeling the non-linear deformation properties of stiff geomaterials. *Geotechnique*, 47(3), 563-580.

Kuwano, R. and Jardine, R.J. 2002. On the application of cross-anisotropic elasticity to granular materials at very small strains. *Geotechnique*, 52(10), 727-749.

Mindlin, R.D. and Deresiewicz, H. 1953. Elastic sphere in contact under varying oblique forces. *J. Appl. Mech., ASME*, 20(3), 327-344.

Oda, M. and Nakayama, H. 1998. Introduction of inherent anisotropy of solids in the yield function. *Micromechanics of Granular Materials*, Elsevier, Amsterdam, 81-90.

Walton, O.R. and Braun, R.L. 1986. Viscosity, Granular-temperature and Stress Calculations for shearing assemblies of inelastic, friction disks. *Journal of Rheology*, 30(5), 949-980.

Yimsiri, S. and Soga, K. 2000. Micromechanics-based stress-strain behavior of soils at small strains. *Geotechnique,* 50(5), 559-571.